Geomechanics and Engineering, *Vol. 31, No. 2 (2022) 209-222*
https://doi.org/10.12989/gae.2022.31.2.209

Effect of soil condition on the coefficient of lateral earth pressure inside an open-ended pipe pile

Junyoung Ko[1a], Sangseom Jeong[2b] and Hoyoung Seo*[3]

[1]*Department of Civil Engineering, Chungnam National University, 99 Daehak-ro, Yuseong-gu, Daejeon 34134, Republic of Korea*
[2]*School of Civil and Environmental Engineering, Yonsei University, 50 Yonsei-ro, Seodaemun-gu, Seoul 03722, Republic of Korea*
[3]*Department of Civil, Environmental and Construction Engineering, Texas Tech University, 911 Boston Ave., Lubbock, TX 79409, USA*

(*Received March 3, 2022, Revised October 9, 2022, Accepted October 16, 2022*)

Abstract. Finite element analyses using coupled Eulerian-Lagrangian technique are performed to investigate the effect of soil conditions on plugging of open-ended piles in sands. Results from numerical simulations are compared against the data from field load tests on three open-ended piles and show very good agreement. A parametric study focusing on determination of the coefficient of lateral earth pressure (K) in soil plug after pile driving are then performed for various soil densities, end-bearing conditions, and layering conditions. Results from the parametric study suggest that the K value in the soil plug – and hence the degree of soil plugging – increases with increasing soil densities. The analysis results further show that the K value within the soil plug can reach about 63 to 71% of the coefficient of passive earth pressure after pile driving. For layered soil profiles, the greater K values are achieved after pile driving when the denser soil layer is present near the pile base regardless of number of soil layers. This study provides comprehensive numerical and experimental data that can be used to develop advanced theory for analysis and design of open-ended pipe piles, especially for estimation of inner shaft resistance after pile driving.

Keywords: coefficient of lateral earth pressure; coupled Eulerian-Lagrangian technique; degree of soil plugging; end-bearing conditions; open-ended piles; soil conditions

1. Introduction

Open-ended steel pipe piles have been widely used as a foundation system to support offshore structures, such as oil platforms and wind turbines, because of their easier drivability compared to closed-ended pipe piles. Furthermore, open-ended steel pipe piles have become a more attractive option even for onshore structures to resist to extreme event loadings such as seismic event, liquefaction, vessel collision, scour and ice (Brown and Thompson 2015). During the driving of an open-ended pipe pile, soils initially enter an empty space inside the pile and a frictional resistance between the soil and inner surface of the pile develops. As the pile is driven deeper into the soil, the soil inside the pile becomes denser and stiffer and, hence, inner shaft resistance increases until a soil plug is formed. The plugged soil inside the pile prevents additional soil from entering the inside of the pile, known as full plugging. When an open-ended pipe pile is fully plugged, it may behave as if it was closed-ended condition. Consequently, there are situations where a refusal is reached during driving of open-ended pipe piles for offshore projects due to internal soil plug when dense sand layers are encountered (Fattah and Al-Soudani 2016).

It is known that the drivability and the bearing capacity of open-ended piles are highly affected by the degree of soil plugging (Paikowsky 1989, Ko and Jeong 2015, Kodsy and Iskander 2022). Factors influencing the degree of the soil plugging can be generally classified into 1) pile geometry, 2) installation method, and 3) soil condition. According to Szechy (1959), the length of soil plug decreases with the increasing pile diameter for the same penetration depth. The same behavior has been observed by subsequent studies by other researchers (Lehane *et al.* 2005, Yu and Yang 2012, Gudavalli *et al.* 2013). In addition, Klos and Tejchman (1981) stated that the end-bearing capacity of open-ended piles was almost equal to that of closed-ended piles when the pile penetration depth was 17 times the pile internal diameter and deeper; they further reported that the difference between shaft resistance of the open-ended and closed-ended piles was negligible for the pile penetration depth reaching more than 30 times the pile internal diameter.

Open-ended pipe piles are typically installed by either driving or jacking them into the ground. Although the effect of installation methods on soil plugging has not received much attention, limited research studies showed that the jacked piles had a greater tendency to plug than the driven piles (De Nicola and Randolph 1997, Paik and Salgado 2004). According to Brown and Thompson (2015), this is because, for driven piles, the inertial resistance of the soil plug under high downward acceleration of the pile caused by a hammer impact becomes large enough to cause the soil

*Corresponding author, Associate Professor
E-mail: hoyoung.seo@ttu.edu
[a]Assistant Professor
E-mail: jyko@cnu.ac.kr
[b]Professor
E-mail: soj9081@yonsei.ac.kr

Copyright © 2022 Techno-Press, Ltd.

ISSN: 2005-307X (Print), 2092-6219 (Online)

plug to slip. For driven open-ended piles, Brucy *et al.* (1991) described that the soil plug length increased with the decreasing hammer weight and the increasing falling height at a constant driving energy.

Soil conditions also play a major role in the soil plugging. Many researchers investigated the effect of soil condition, mainly relative density of sand, on the degree of soil plugging (Kishida and Isemoto 1977, Kraft 1991, Randolph *et al.* 1992, Paik and Lee 1993, Kikuchi *et al.* 2009). It has been observed that the soil plug length inside the pile increased with the increasing relative density (Paik and Lee 1993, Kikuchi *et al.* 2009, Seo and Kim 2017). Although the previous studies provided general trends between the soil plug length and soil condition, they were based on the results from laboratory-scale model tests and, therefore, findings from the studies may not be directly applicable to field conditions.

Numerical analysis may become a very valuable tool to investigate the effect of soil conditions on the plugging phenomenon under field conditions. However, modelling the driving process of open-ended pipe piles deep into the ground is a large deformation problem and impose its own numerical challenges due to severe mesh distortions and moving boundaries. To overcome these limitations, the Coupled Eulerian-Lagrangian (CEL) method has been applied. For example, Ko *et al.* (2016) performed large-deformation numerical analyses using the CEL technique for field-scale piles to investigate various factors that influence soil plugging. However, their study mainly focused on the validation of the numerical model and covered overall response of open-ended piles for different pile diameters and driving energies, rather than investigating the effect of soil condition on plugging behavior in greater details. Despite the widespread use of open-ended pipe piles, the change of stress state, especially the radial stress, of the soil plug inside the pile is still poorly understood.

This study presents results from large-deformation numerical analyses focusing on the effect of soil conditions on plugging of open-ended piles using the CEL technique. The numerical model used in this study is validated through comparison against results from high-quality field load tests. Effects of model parameters related to soil conditions such as friction angles, end-bearing conditions, and soil layering profiles are studied and discussed. Particular emphases are placed on investigations of the coefficient of lateral earth pressure (K) after the pile driving for various soil conditions.

2. Soil plugging of open-ended piles

2.1 Degree of soil plugging

The plugging of open-ended piles means that the space inside is plugged up by soil, restricting or preventing additional soil from entering the inside of the pile. As the degree of soil plugging increases, the open-ended piles may behave as if those were closed-ended conditions. Qualitatively, the degree of soil plugging of open-ended piles can be described as unplugged, partially plugged, or fully plugged condition. Typically, the degree of soil plugging is quantified using the plug length ratio (*PLR*) or incremental filling ratio (*IFR*). The *PLR* and *IFR* are defined as follows

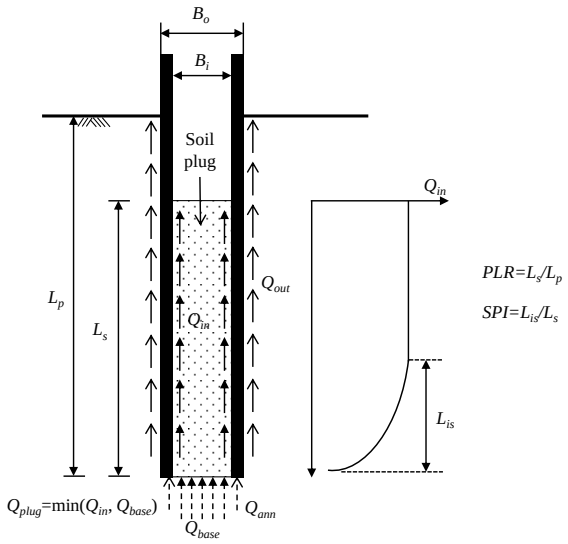

Fig. 1 Components of bearing capacity for open-ended pile and definitions of plug length ratio (*PLR*) and soil plugging index (*SPI*)

$$PLR = \frac{L_s}{L_p} \tag{1a}$$

$$IFR = \frac{\Delta L_s}{\Delta L_p} \tag{1b}$$

where L_s = soil plug length, L_p = pile penetration depth, ΔL_p = increment of pile penetration depth, and ΔL_s = increment of soil plug length corresponding to an increment of pile penetration depth ΔL_p.

Forces acting on an open-ended pile are composed of outer shaft resistances (Q_{out}), inner shaft resistance (Q_{in}), resistance of annular pile base (Q_{ann}), and end-bearing resistance (Q_{base}) of the soil beneath the base of the soil plug, as shown in Fig. 1. It has been reported that the contribution of top portion of the soil plug to the inner shaft resistance Q_{in} is minimal, and most of the inner shaft resistance is mobilized near the pile tip under the ultimate load (Paikowsky 1990, Igoe *et al.* 2008, 2010, Ko and Jeong 2015) (refer to load-distribution curve in Fig. 1). The level of the inner shaft resistance mobilization can be quantified using soil plugging index (*SPI*), defined as

$$SPI = \frac{L_{is}}{L_s} \times 100\% \tag{2}$$

where L_s is the soil plug length and L_{is} is the length of the soil plug along which inner shaft resistance is mobilized.

2.2 Current design practice

Several design methods that use *PLR* or *IFR* to estimate the ultimate capacity of open-ended piles have been suggested (Paik and Salgado 2003, Lehane *et al.* 2005,

Gudavalli *et al.* 2013). However, the current design practice is based on equilibrium of static forces acting on the pile (American Petroleum Institute 2011). When an open-ended pile is unplugged, the inner frictional resistance Q_{in} is smaller than the end-bearing resistance Q_{base} beneath the soil plug and, therefore, additional soils enter inside the pile. This means that only Q_{in} is fully mobilized as resistance. On the other hand, when fully plugged, Q_{in} is greater than Q_{base} and additional soils cannot enter, meaning that only Q_{base} is fully mobilized as resistance. Consequently, the ultimate capacity (Q_{ult}) of the open-ended pile is the summation of 1) the outer shaft resistances (Q_{out}), 2) resistance of annular pile base (Q_{ann}), and 3) soil plug resistance (Q_{plug}), which is the smaller value of Q_{in} and Q_{base}, and expressed as follows

$$Q_{ult} = Q_{out} + Q_{ann} + Q_{plug} = q_{s,out}A_{s,out} + q_bA_{b,ann} + q_{s,in}A_{s,in} \quad \text{(unplugged)} \tag{3a}$$

$$Q_{ult} = Q_{out} + Q_{ann} + Q_{plug} = q_{s,out}A_{s,out} + q_bA_{b,ann} + q_bA_{b,plug} \quad \text{(plugged)} \tag{3b}$$

where $q_{s,out}$ = outer unit shaft resistance; $A_{s,out}$ = outer surface area of pile-soil interface (= $\pi B_o L_p$ where B_o is outer pile diameter); q_b = unit end bearing resistance; $A_{b,ann}$ = annular area of pile base; $q_{s,in}$ = inner unit shaft resistance; $A_{s,in}$ = inner surface area of pile-soil interface (= $\pi B_i L_s$ where B_i is inner pile diameter); and $A_{b,plug}$ = cross-sectional area of soil plug.

The unit shaft resistance (q_s) of piles driven in sands can be computed from the horizontal effective stress (σ'_h) acting on the pile surface and the frictional properties between the pile and soil interface as follows

$$q_s = \sigma'_h \tan\delta = K\sigma'_v \tan\delta \tag{4}$$

where K = coefficient of lateral earth pressure (= σ'_h/σ'_v); σ'_v = vertical effective stress; and δ = soil-pile interface friction angle. The K and tanδ terms are often incorporated together as shaft friction factor β (= Ktanδ), and Eq. (4) then becomes $q_s = \beta\sigma'_v$. According to the American Petroleum Institute (2011), β values vary between 0.37 and 0.56 for open-ended pipe piles driven in medium dense to very dense sands.

The API (2011) guideline further suggests that the unit end bearing resistance for piles installed in sands be obtained as follows

$$q_b = N_q\sigma'_{vb} \tag{5}$$

where σ'_{vb} = vertical effective stress at the pile tip; and N_q = end bearing factors ranging between 20 and 50 for medium dense to very dense sands.

Current practice for geotechnical design of open-ended piles uses Eqs. (4) and (5) to compute the unit shaft resistance and unit end bearing resistance and then takes the smaller value of the capacities computed from Eqs. (3(a)) and (3(b)) as the ultimate capacity. During this process, it is commonly assumed that the inner and outer unit shaft resistances are the same ($q_{s,in}$ = $q_{s,out}$ = q_s). Further, it is assumed that the K value remains constant with respect to depth for the same soil condition. In reality, however, the K values of the soil plug at the end of the pile driving depend on the initial density of sands, distance from the pile tip, and degree of soil plugging, and therefore differ from those of outside soil. Several researchers (Paik and Lee 1993, De Nicola and Randolph 1997, Jeong *et al.* 2015) suggested methodologies for evaluating inner shaft resistance considering the development of K values after the pile driving. However, it is extremely difficult to accurately determine the inner shaft resistance of an open-ended pipe pile because the K value of the soil plug after the completion of the pile driving cannot be measured in routine piling (Malhotra 2002).

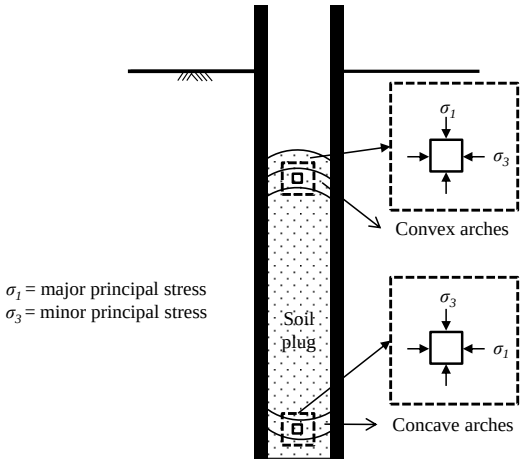

Fig. 2 Arching mechanism of soil plug for open-ended piles (modified after Paikowsky (1990))

2.3 Development of lateral stress in the soil plug

Paikowsky (1989, 1990) conceptually described the mechanism of the build-up of lateral stresses in the soil plug using arching effect. According to Paikowsky (1989), when a pile is moving downward during the driving (equivalent to the upward movement of the soil), soils resisting such downward movement should naturally form a concave arch (downward). However, for the open-ended pipe piles, the frictions between soil and inner surface of the pile are very small during the initial penetrations at shallow depths and, therefore, soils cannot develop enough resistances to the upward pushing forces. Consequently, the concave soil arches fail and soils continuously flow upward, leading to reverse shapes of convex arches near the top of soil plug (refer to Fig. 2). This implies that the vertical stress along the centerline of the pile is a major principle stress and K value is smaller than 1 where the convex arches are observed.

Upon further penetration, the inner frictional resistances increase continuously because soil plugs become denser. At a certain depth below the top of the soil plug, the resistance will become large enough to resist to the upward pushing force and the arch will not be destroyed. Paikowsky (1989) called the portion of the soil plug in this stress state as a transition layer and argued that a hydrostatic stresses (K = 1) will exist in the transition layer.

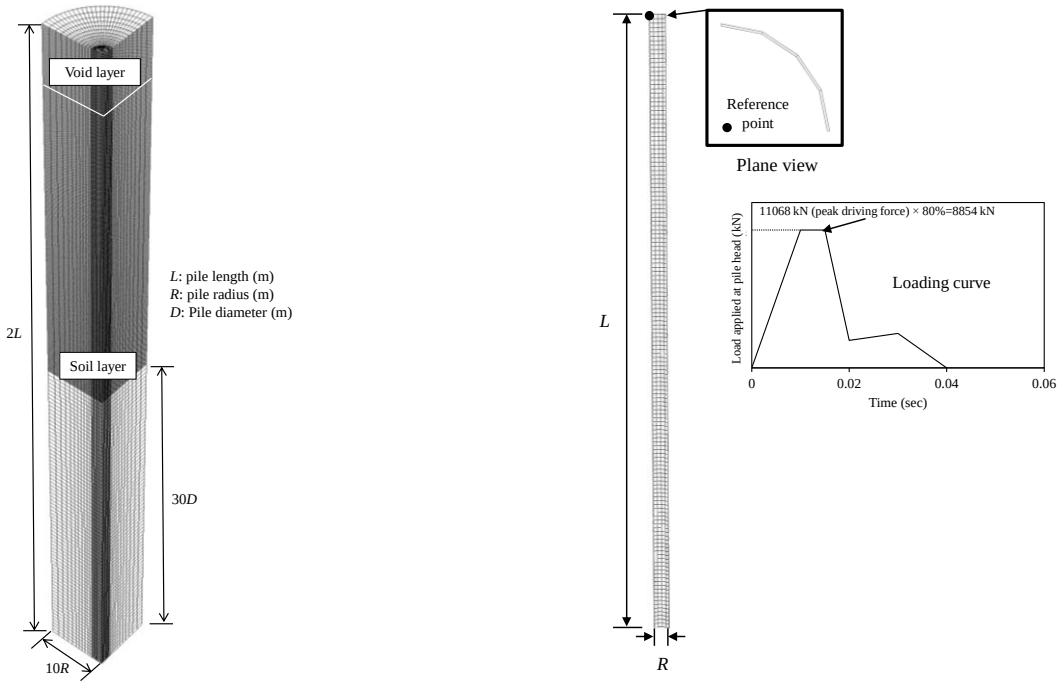

(a) Soil domain (b) Pile domain and loading curve simulating hammer blow

Fig. 3 Finite element mesh for CEL analysis

Further penetration and the build-up of lateral stresses will provide sufficiently large resistances to the upward pushing forces and allow the development of concave arch near the bottom of the soil plug (refer to Fig. 2). Paikowsky (1989) stated that these arches might transfer lateral stresses at the pile-soil interface that are greater than the vertical stresses, leading to K value larger than 1 where the concave arches are observed.

In order to accurately predict the inner shaft resistance of open-ended piles, it is necessary to obtain the stress state in the soil plug after driving. However, as Malhotra (2002) stated, "the lack of knowledge of the state of stress in the soil plug makes it impossible (so far) to determine the actual coefficient of [lateral] earth pressure." Investigating the coefficient of lateral earth pressure of the soil plug through large number of full-scale load tests for various conditions may not be feasible for practical and economical reasons. As an alternative solution, the authors numerically investigate the response of soil plug in various soil conditions in this study, focusing on estimation of coefficient of lateral earth pressure at the end of the pile driving, using the CEL technique.

3. Coupled-Eulerian-Lagrangian finite elements analysis

Traditional numerical approaches based on the Lagrangian coordinates have limitations when performing large-deformation problems due to contact problems and severe mesh distortions. To overcome these limitations, the CEL method has been recently applied in geotechnical engineering. The CEL method has advantages of both the Lagrangian and the Eulerian coordinates.

Because the CEL method does not require re-meshing, severe mesh distortions causing numerical instability do not occur in a CEL analysis (Qiu *et al.* 2011, Tho *et al.* 2012, Ko *et al.* 2016). Due to such advantages, the CEL method has been widely used to investigate the large deformation problems such as offshore anchoring techniques (Tho *et al.* 2012, Yi *et al.* 2012, Tho *et al.* 2014, Bienen *et al.* 2015, Kim *et al.* 2015a, b, Zhao and Liu 2015, Lai *et al.* 2020), debris flow (Lee and Jeong 2018, Lee *et al.* 2019), driven piles (Pucker and Grabe 2012, Tho *et al.* 2014, Ko *et al.* 2016, Chen *et al.* 2020), static cone penetration process (Gupta *et al.* 2016), impact of high-speed water jet (Hsu *et al.* 2013), and TBM excavation (Kim and Jeong 2021) .

In this study, the CEL method in ABAQUS/Explicit (Dassault Systemes 2018) is employed to simulate the response of soil plug in open-ended piles during driving. The pile and soil are considered as the Lagrangian and Eulerian coordinates, respectively. The Eulerian domain for soil is composed of two layers: soil layer and void layer. The void layer is provided so that the soil can be heaved and moved into the empty element and has zero strength and stiffness (Ko *et al.* 2016).

Fig. 3 shows a typical finite element (FE) mesh and boundary sizes of the soil and pile for the quarter domain because of the symmetrical modelling. The radial boundary is fixed at 10R (where R is a pile radius) from the center of the pile. Also, the bottom boundary is set at a distance L (where L is a pile length) below the pile base, which resulted in a minimum distance of 30 pile diameter which is deemed sufficient to avoid boundary effects (Ko *et al.* 2016).

The symmetric boundary conditions are imposed on the two planes of symmetry by prescribing a zero flow velocity normal to these planes. Also, no radial flow is permitted at

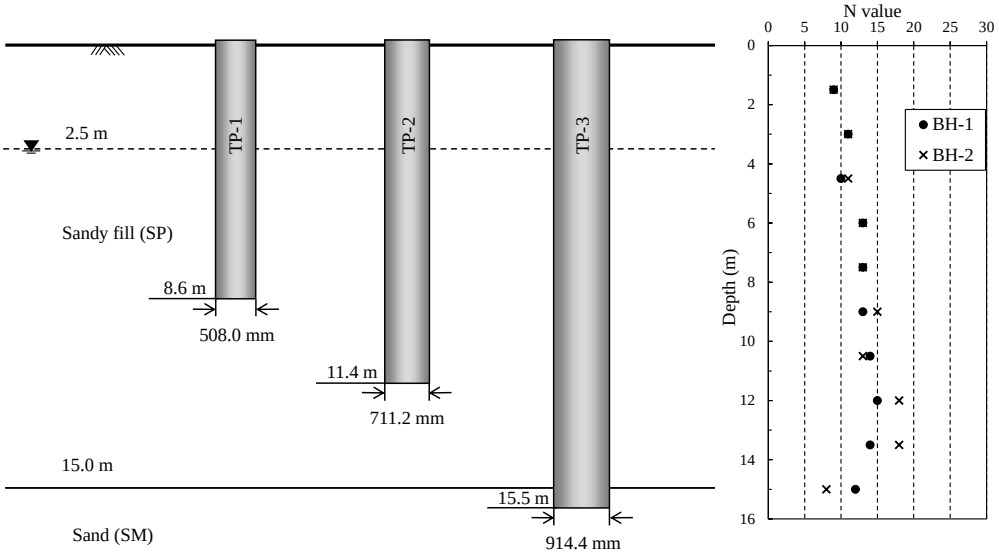

Fig. 4 Soil profiles with SPT results and geometries of instrumented piles

the curved face representing the far-field boundary, and no vertical flow is permitted at the base of the model (Tho *et al.* 2012, Ko *et al.* 2016). The pile and soil are represented as the eight-noded Lagrangian brick elements (C3D8R) and eight-noded Eulerian brick elements (EC3D8R), respectively.

The general contact element method based on the penalty contact method in ABAQUS is applied to interface between Eulerian and Lagrangian coordinates in this study. The master surface tracks nodes in the slave surface using a search algorithm known as the contact tracking algorithm (Tolooiyan and Gavin 2011, Ko *et al.* 2016). The interface element modelled by the Coulomb's frictional model is employed to simulate the pile-soil interface. The friction coefficient μ of 0.3 is chosen in this analysis following Randolph and Wroth (1981).

The geostatic stress is applied in a predefined step to consider initial equilibrium state. After applying the initial step for geostatic stress, a pile driving force is imposed at the pile head to simulate the pile installation process. Although very limited studies have been performed on modelling of the impact pile driving using FEM due to the numerical challenges, Mabsout *et al.* (1995, 1999) successfully implemented pile driving process into FEM by applying a "forcing function" at the pile head using the measured force profile by Goble *et al.* (1980). In Mabsout *et al*'s study (1995, 1999), the peak force of 2,500 kN measured by pile driving analyzer (PDA) was reduced by 20% to avoid excessive tensile stress in the pile, and then the reduced peak force was applied at the pile head as a transient force for a duration of 0.04 sec in the FEM analysis. The present study follows the same approach but with a greater peak force because the pile diameter and soil stiffness employed in this study are greater than those in the study by Mabsout *et al.* (1995, 1999).

Maximum rated energies of pile driving hammers that are commonly used to install 0.5-m-diameter open-ended piles in sandy soils – the conditions used for parametric study in this paper – vary from about 60 kNm to 170 kNm (Gudavalli *et al.* 2013, Caltrans 2015, Ko and Jeong 2015). Considering that the efficiency of pile driving hammers ranges between 0.5 and 0.95 depending on hammer types (Rauche 2000), a maximum driving energy of 100 kNm (i.e., equivalent to a hammer weight of 100 kN with a falling height of 1 m) is selected for this study. The maximum energy is first converted to a peak force (11,068 kN) based on Newton's second law and then reduced by 20% as done by Mabsout *et al.* (1995, 1999). Finally, a discrete hammer blow is applied by a loading curve with the reduced peak force (8,854 kN) for a duration of 0.04 sec. Fig. 3(b) shows the loading curve employed in this study.

4. Validation against results from field load tests

4.1 Field load tests

Ko and Jeong (2015) performed full-scale field load tests, both dynamic and static axial compression load tests, on three open-ended steel pipe piles instrumented with strain gauges at the Kwangyang Substituted Natural Gas (SNG) plant site in Korea. Outer diameters of three test piles (TP-1, TP-2, and TP-3) were 508, 711.2, and 914.4 mm, respectively. Subsurface profile at the test site consisted of a loose to medium dense sandy fill from the ground surface to a depth of 15 m. The standard penetration number (N value) of the sandy fill ranged from 8 to 18. Below the sandy fill layer, a medium dense sand layer was encountered with SPT N values ranging from 12 to 27. The three test piles were driven to depths ranging from 8.6 to 15.5 m. Fig. 4 shows the soil profiles and geometries of instrumented test piles. Based on laboratory test results, the specific gravity (G_s), the coefficient of uniformity (C_u), and the coefficient of curvature (C_c) of the sandy fill were determined to be 2.70, 2.00, and 1.01, respectively. According to the Unified Soil Classification System

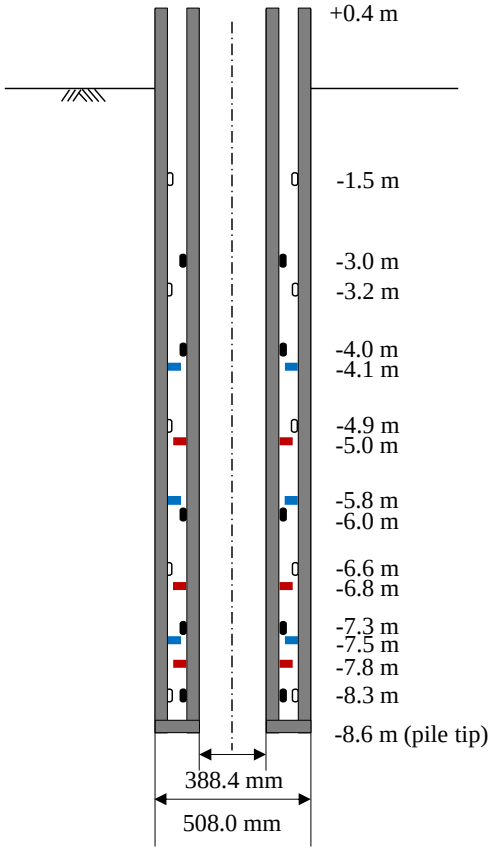

(a) TP-1

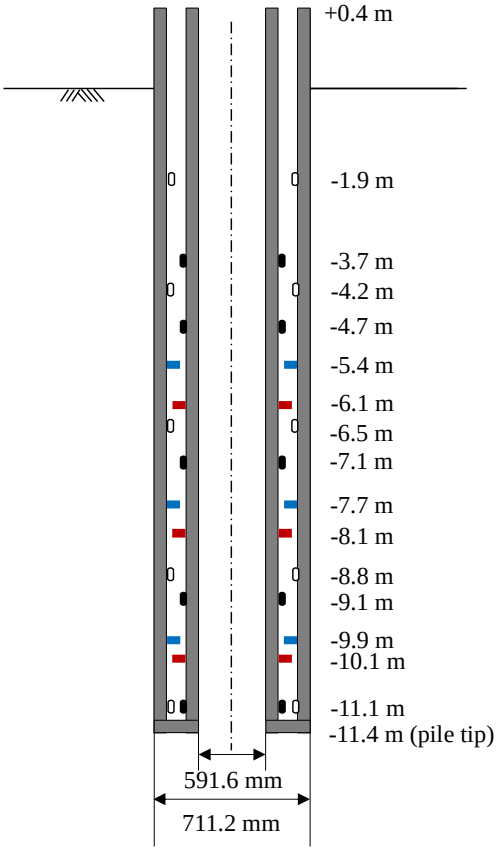

(b) TP-2

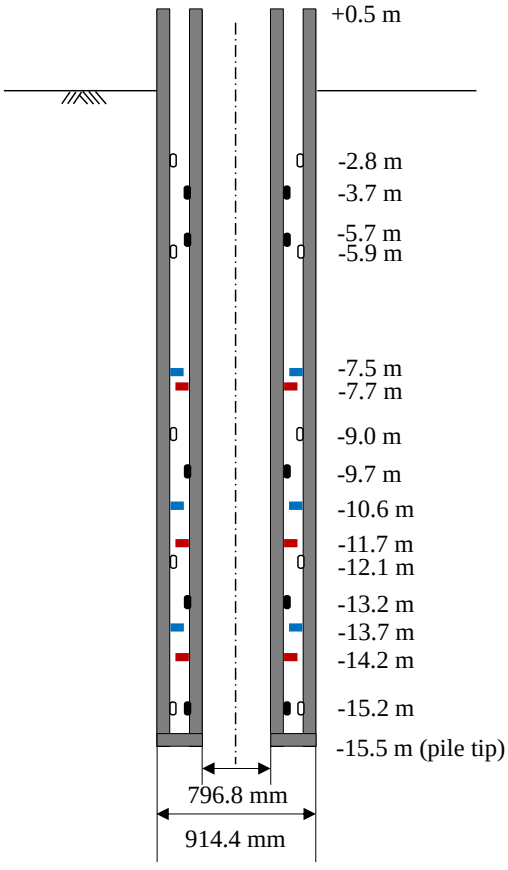

(c) TP-3

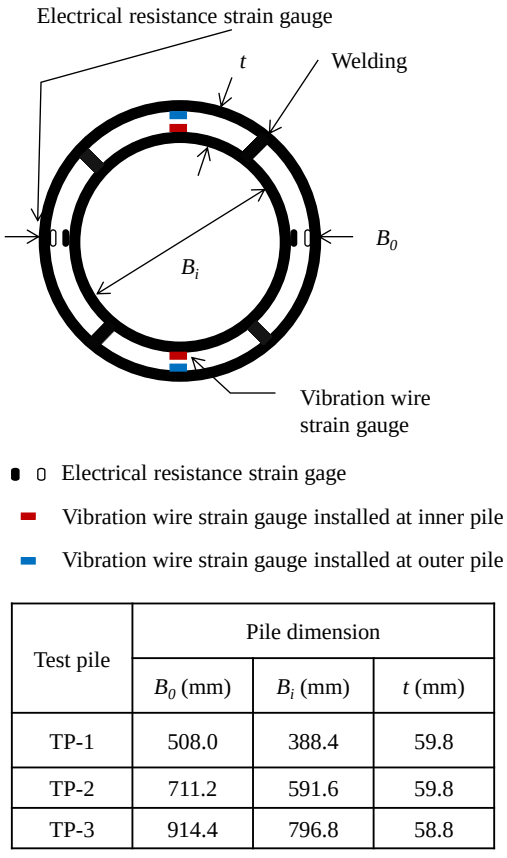

Test pile	Pile dimension		
	B_0 (mm)	B_i (mm)	t (mm)
TP-1	508.0	388.4	59.8
TP-2	711.2	591.6	59.8
TP-3	914.4	796.8	58.8

(d) cross section

Fig. 5 Double-walled instrumented piles

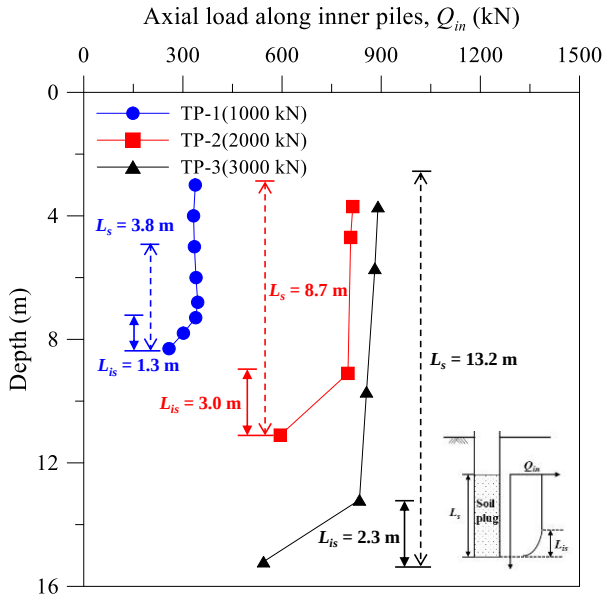

Fig. 6 Axial load transfer curves of inner piles along the soil plug lengths under ultimate loads

(USCS), the sandy fill from ground surface to 15 m was classified as SP, and the medium dense sand below the fill was classified as SM.

To measure various components of bearing capacity of open-ended piles such as outer shaft resistance (Q_{out}), the inner shaft resistance (Q_{in}), and the annulus capacity (Q_{ann}), the test piles were prefabricated as double-walled pipe piles (two concentric pipes with inner one having slightly smaller diameter than the outer one), as shown in Fig. 5. A total of 20 electrical resistance strain gauges and 12 vibration wire strain gauges were instrumented along outside of the inner pile and inside of the outer pile to measure the inner (Q_{in}) and outer shaft resistances (O_{out}).

To calculate the *PLR*, the soil plug lengths (L_s) were measured at the end of pile driving. The measured soil plug lengths of TP-1, TP-2, and TP-3 were 3.8 m, 8.7 m, and 13.2 m, respectively, at final penetration depths, corresponding to *PLR* values of 0.44, 0.76, and 0.85, respectively. Axial loads along the pile were obtained from the strain gauge measurements, and Fig. 6 shows distributions of the axial loads along the inner piles under the ultimate loads (further details on the results from the pile load tests can be found in Ko and Jeong (2015)). For all cases, most of the inner shaft resistance Q_{in} is mobilized near the pile tip under the ultimate load. Based on the axial load distribution curves, the mobilized soil plug lengths L_{is} of TP-1, TP-2, and TP-3 were determined to be 1.3, 2.0, and 2.3 m under the ultimate loads, respectively, corresponding to SPI values of about 34%, 23%, and 17%, respectively.

4.2 Comparisons with field load tests

To validate the CEL modelling, results from numerical simulations are compared with the field load tests data reported by Ko and Jeong (2015) both quantitatively and qualitatively. The input parameters for model validation are summarized in Table 1.

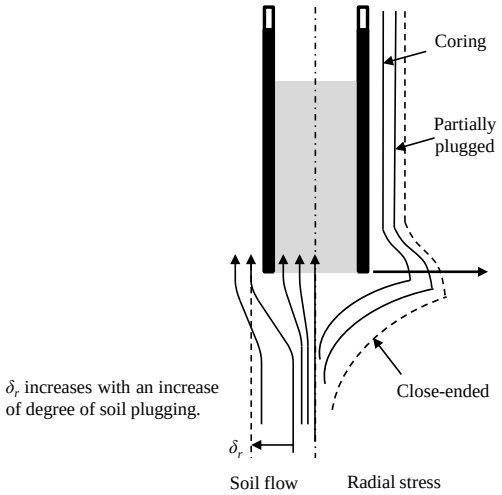

(a) Schematic plot of soil flow and radial stress for open-ended piles (modified after White *el al.* (2005))

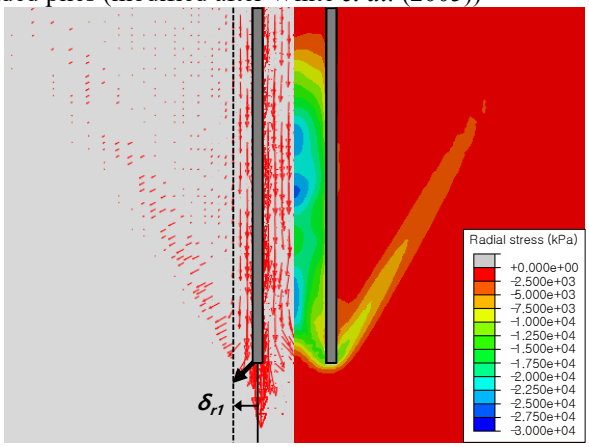

(b) TP-1 (small-diameter pile)

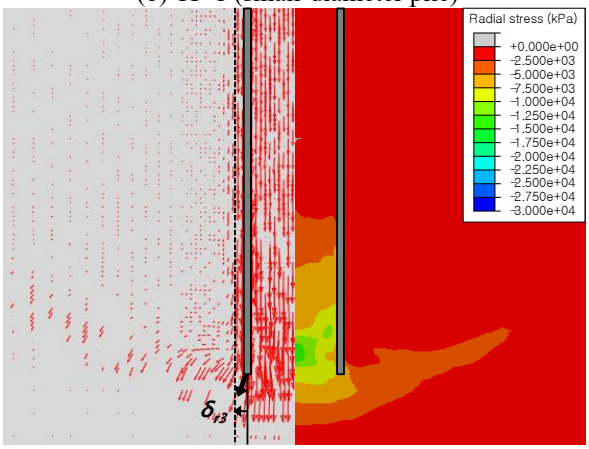

(c) TP-3 (large-diameter pile)

Fig. 7 Comparison between theoretical mechanism of plugging effect and numerical analysis

Table 1 Input parameters for validation of numerical model (Kwangyang full-scale tests)

Type	Model	γ_t (kN/m^3)	E (MPa)	ϕ (degrees)	c (kPa)	Poisson's ratio, ν
Sand	Mohr-Coulomb	17.6	13.5	32	0	0.3
Pile	Linear Elastic	75.0	210,000	-	-	0.2

Table 2 Comparisons of *PLR* and *SPI*

Test Pile	*PLR*			*SPI* (%)		
	CEL	Measured	CEL / Measured	CEL	Measured	CEL / Measured
TP-1	0.52	0.44	1.18	40	34	1.18
TP-2	0.75	0.76	0.99	23	23	1.00
TP-3	0.90	0.85	1.06	13	17	0.76

White *et al.* (2005) explained possible trajectories of soil particles flow and distribution of radial stress during driving process of open-ended piles. As shown in Fig. 7(a), radial stresses near the pile tip increases with an increase of degree of soil plugging because larger radial displacements are required for the same amount of penetration. Similarly, the relative displacement of radial soil flow (δ_r), defined as the amount radial displacement from its initial location, depends on the degree of soil plugging. The δ_r of open-ended piles increases with an increase of degree of soil plugging, and the δ_r approaches that of closed-ended piles when fully plugged (White *et al.* 2005).

Since radial displacements and changes of stress state in soils could not be measured from the full-scale field tests, qualitative validations are made against the schematic plot of Fig. 7(a). Figs. 7(b) and 7(c) represent the plots of velocity vector and radial stress from the CEL analyses for TP-1 (B_o = 508 mm) and TP-3 (B_o = 914.4 mm), respectively. As seen in Figs. 7(b) and 7(c), the relative displacement of radial soil flow δ_{r1} of TP-1 is greater than that (δ_{r3}) of TP-3. In addition, the magnitude of radial stress and its influence zone for TP-1 are greater than those of TP-3. These results are well in agreement, qualitatively, with the schematic plot shown in Fig. 7(a). These results further indicate that the degree of soil plugging of the open-ended piles increases with a decrease in the pile diameter in the same soil conditions, which is consistent with the previous studies (Szechy 1959, Klos and Tejchman 1981, Paikowsky 1989, Gudavalli *et al.* 2013, Seo and Kim 2017).

The effect of pile diameter on the degree of soil plugging becomes more evident in quantitative comparison. Table 2 presents comparisons of *PLR* and *SPI* values obtained from the CEL analyses with those measured in the field tests. Both the CEL analyses and field tests suggest *PLR* increases with increasing diameter, indicating decrease of degree of soil plugging. The ratio of predicted *PLR* from the CEL analysis to the measured value ranges 0.99 to 1.18. On the other hand, both the CEL analyses and field tests suggest *SPI* values decrease with increasing pile diameter, indicating decrease of degree of soil plugging. The ratio of predicted *PLR* from the CEL analysis to the measured value ranges from 0.76 to 1.18. Both qualitative and quantitative comparisons suggest that the CEL model employed in this study is reasonable enough to conduct a parametric study.

5. Parametric studies

To investigate the effect of soil conditions on the plugging behavior of open-ended piles, a series of CEL analyses were performed for various 1) soil densities, 2) end-bearing conditions, and 3) soil layering cases. An open-ended steel pipe pile with an outer diameter of 0.5 m and a wall thickness of 10 mm was considered in the parametric study. The pile was driven to a depth of 15 m using the forcing function described earlier in the numerical modelling section. The coefficient of lateral earth pressure at rest (K_0) before pile driving was taken as 0.4 for all analyses. In this analysis, the variation of the coefficient of lateral earth pressure (K) acting on the inner surface of the pile is employed as an indicator to investigate the relationship between the degree of soil plugging and the influence factors. Table 3 summarizes the input parameters used for the parametric studies.

5.1 Effect of soil density

The effect of soil densities on plugging behavior was investigated by considering loose, medium dense, and dense sands in the parametric study. Elastic moduli (E) for the loose, medium dense, and dense sands were assumed to be 12.5, 22.5, and 32.5 MPa, respectively; similarly, peak friction angles (ϕ) were assumed to be 26, 34, and 39.5 degrees, for loose, medium dense, and dense sands, respectively (refer to Table 3). Poisson's ratio was taken as 0.3 for all soil conditions.

Fig. 8(a) shows the coefficient of lateral earth pressure K acting on the inner surface of the pile versus the distance from the pile tip (L_{tip}) for various soil conditions. Medium dense sand and dense sand show that K values are close to initial value (K_0 = 0.4) or slightly larger than the initial value but still smaller than 1 for upper portion of the soil plug. The K values then start to increase and reach maximum values that are greater than 1 near the pile base and decrease toward the pile base. Such a trend is in very good agreement with the aforementioned conceptual model proposed by Paikowsky (1989). The loose sand shows similar behavior although the K values for the upper portion of the plug is close to 1.

The largest K values within the soil plugs were 1.6, 2.5, and 3.2 for loose, medium dense, and dense sands, respectively. Lengths of soil plug L_s at the end of pile driving process (*i.e.*, L_p = 15 m) obtained from the CEL analysis were 6.75, 9.75, and 10.95 m for loose, medium dense, and dense sands, respectively; this corresponds to *PLR* values of 0.45, 0.65, and 0.73 for loose, medium dense, and dense sands, respectively. The trend of increasing *PLR* with increasing density of soil has been observed in many experimental studies (Paik and Lee 1993, Paik and Salgado 2003, Kikuchi *et al.* 2009, Seo and Kim 2017), and the CEL analysis results from this study support that. Also, for medium dense and dense sands, K values along the top portions of the soil plug are smaller than 1 whereas those near the pile tip are greater than 1.

The portions of the Fig. 8(a) where K values start to increase significantly and therefore mostly exceed 1 are plotted separately in Fig. 8(b); these portions of the curves are essentially equivalent to the lengths of mobilized soil plug lengths L_{is} for each soil condition. Note that the distance from the pile tip on the vertical axis in Fig. 8(b) is

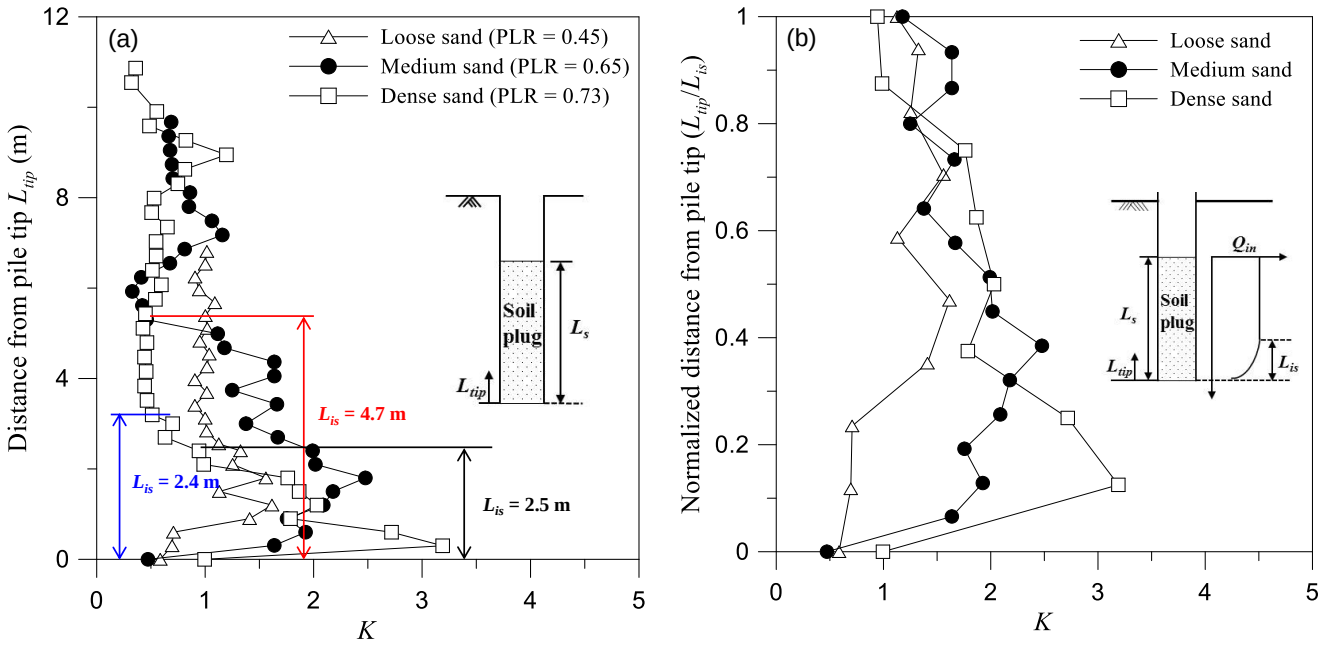

Fig. 8 Variations of K in the soil plug for various soil densities versus (a) distance from pile tip L_{tip} and (b) normalized distance from pile tip with respect to the mobilized soil plug L_{tip}/L_{is}

Table 3 Input parameters for the parametric studies

Parameter	Case	Remarks	E (MPa)	E_E (MPa)	ϕ (deg.)	ϕ_E (deg.)	c (kPa)	Poisson's ratio, v
Density	Sand1	Loose sand	12.5	-	26.0	-	0.0	0.30
	Sand2	Medium sand	22.5	-	34.0	-	0.0	0.30
	Sand3	Dense sand	32.5	-	39.5	-	0.0	0.30
End-bearing condition	Floating	Floating pile	22.5	-	34.0	-	-	0.30
	0 m	0 m embedded	22.5	32.5	34.0	39.5	-	0.30
	1.5 m	1.5 m embedded	22.5	32.5	34.0	39.5	-	0.30
	3.0 m	3.0 m embedded	22.5	32.5	34.0	39.5	-	0.30
Layering condition	SL1 – SL6 (See Fig. 11)	Loose sand	12.5	-	26.0	-	0.0	0.30
		Medium sand	22.5	-	34.0	-	0.0	0.30
		Dense sand	32.5	-	39.5	-	0.0	0.30

normalized with respect to L_{is} (values of L_{is} were 2.5, 4.7, and 2.4 m for loose, medium dense, and dense sands, respectively, as shown in Fig. 8(a)). Although no obvious trend on how the K values vary with soil densities along the entire length of L_{is} is identified, it is observed that the K values increase with increasing relative density near the pile tip ($0 < L_{tip}/L_{is} < 0.3$). The maximum K values observed for each soil density were 1.6, 2.5, and 3.2 for loose, medium dense, and dense sands, respectively, and these K values correspond to about 63%, 70%, and 71% of the coefficient K_p of passive earth pressure, respectively. In fact, Kraft (1991) argued that the lateral earth pressure may approach passive conditions as the advancing pile displaces the soil, and this study supports his argument.

5.2 Effect of end-bearing condition

Driven piles are often tipped into bearing stratum. To investigate the effect of the end-bearing conditions on the plugging effect, additional analyses were performed in a two-layered soil with the upper layer with E = 22.5 MPa and ϕ = 34° and the lower end bearing layer E_E = 32.5 MPa and ϕ_E = 39.5° (refer to Table 3). A total of four cases were analyzed: 1) a friction pile with the pile tip located 1.5 m above the bearing layer (*i.e.*, $L_p = z_{bearing} - 1.5$ m, where L_p = pile penetration depth and $z_{bearing}$ = depth to the top of the bearing layer below ground surface), 2) an end-bearing pile directly resting on the bearing layer ($L_p = z_{bearing}$), 3) an end-bearing pile with the pile tip embedded 1.5 m into the bearing layer ($L_p = z_{bearing} + 1.5$ m), and 4) an end-bearing pile with the pile tip embedded 3 m into the bearing layer ($L_p = z_{bearing} + 3$ m). Fig. 9 illustrates these four cases.

Fig. 10 presents the distribution of the K along the normalized distance from pile tip, L_{tip}/L_{is}, for four different end-bearing conditions. The end-bearing conditions show very little difference in K values for the bottom one third of the mobilized soil plug ($0 < L_{tip}/L_{is} < 0.3$) and top one third ($0.7 < L_{tip}/L_{is} < 1.0$). However, for the middle portion of the mobilized soil plug ($0.3 < L_{tip}/L_{is} < 0.7$), it is observed that the K values generally increase with the increasing

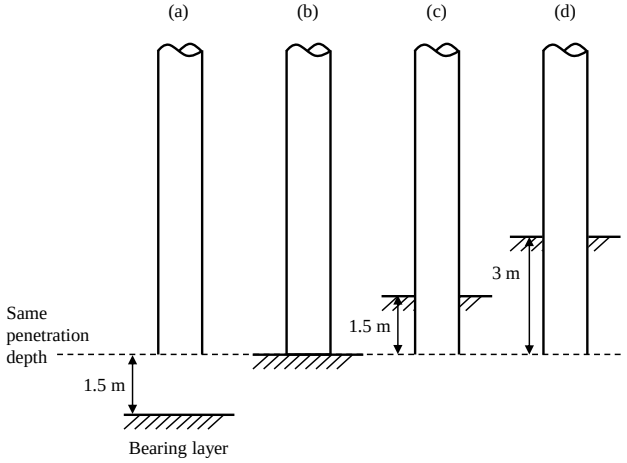

Fig. 9 Piles with different end-bearing conditions: (a) floating pile, (b) 0 m embedded, (c) 1.5 m embedded and (d) 3 m embedded

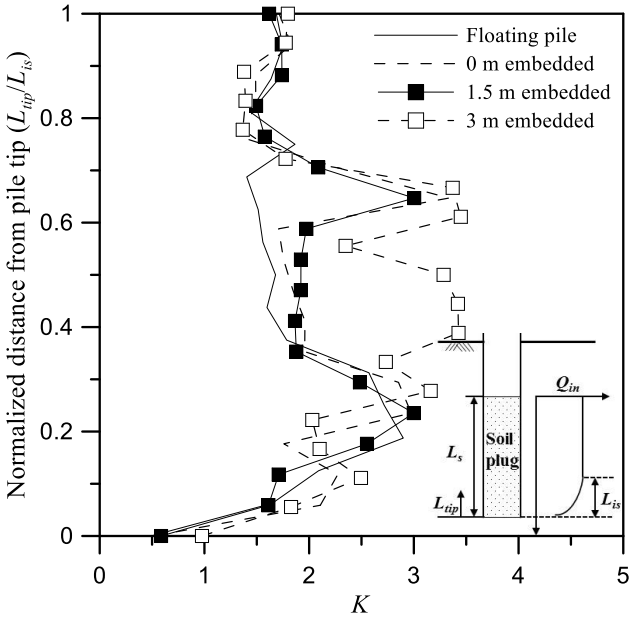

Fig. 10 Variations of K in the soil plug for various end-bearing conditions versus normalized distance from pile tip L_{tip}/L_{is}

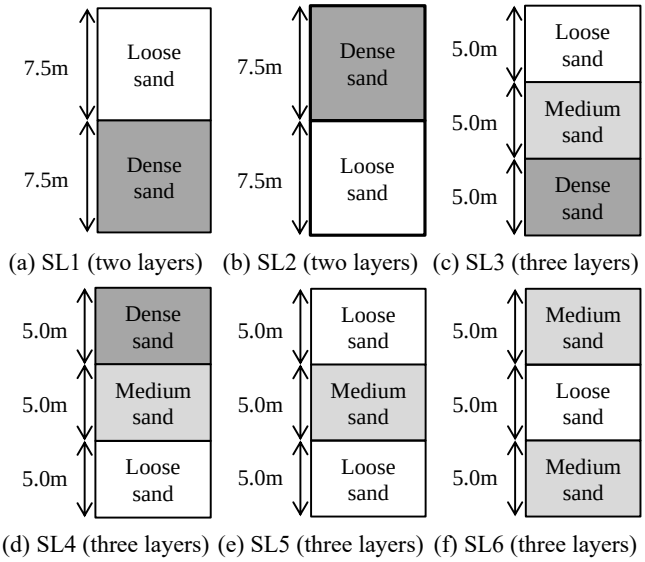

Fig. 11 Soil layering profiles for parametric study

embedment length in the bearing layer (i.e., $L_p - z_{bearing}$), indicating that the end-bearing piles have more influence on the degree of soil plugging than the friction piles. As the embedment length in the bearing layer ($L_p - z_{bearing}$) increases, more amount of denser (or stiffer) soils enters the inside of the pile during the pile penetration and, therefore, it is likely that the degree of soil plugging becomes higher. These results are consistent with the findings from the parametric study on the effect of the soil density in the previous section.

5.3 Effect of soil layering

This section presents the effect of the soil layering on the plugging effect. Fig. 11 shows the six layering profiles considered in the parametric study. Profiles SL1 (two layers) and SL3 (three layers) represent ground conditions with soil density increasing with depth, whereas Profiles SL2 (two layers) and SL4 (three layers) represent ground conditions with the density decreasing with depth. The Profile SL5 (three layers) represents loose sand layers with a medium dense layer in between them. Similarly, Profile SL6 (three layers) represents medium dense sand layers with a loose sand layer in between them.

Fig. 12(a) presents the variations of K values for the two-layer profiles (SL1 and SL2). The maximum value of K for SL1 is 2.83, whereas that for SL2 is 2.07. Fig. 12(b) shows the variation of K for three-layer profiles; the maximum K for SL3 is 3.21, whereas that for SL4 is 2.06. Whether the condition is two-layered or three-layered, it is observed that the greater K values are obtained when the density of the lower layer is higher. Since all the piles were penetrated to the same depths, this result indicates that the K values are greater when the pile tip is in dense soils.

Fig. 12(c) shows the variation of the K values for the soil conditions where the density increases with increasing depth (SL1 and SL3). Interestingly, both cases show two local maximum values. The K values initially increase with increasing L_{tip}/L_{is} and have local maximum values at L_{tip}/L_{is} = 0.3 – 0.4. The K values then decrease and have local minimum values at about L_{tip}/L_{is} = 0.5. After reaching the local minimum values, the K values increase again showing the second local maximum values at L_{tip}/L_{is} becomes about 0.7. On the other hand, Fig. 12(d) that represents the soil conditions where the density decreases with increasing depth (SL2 and SL4) does not show this behavior, having only one local maximum at the location near the bottom portion of the mobilized soil plug.

Fig. 12(e) shows the distributions of the K values for SL5 and SL6, where one layer is sandwiched by the other two layers with different densities. The maximum K values were 2.59 and 3.39 for SL5 and SL6, respectively. As was observed in Figs. 12(a) and 12(b), the maximum K value within the mobilized soil plug is larger when the pile tip is located in denser soils.

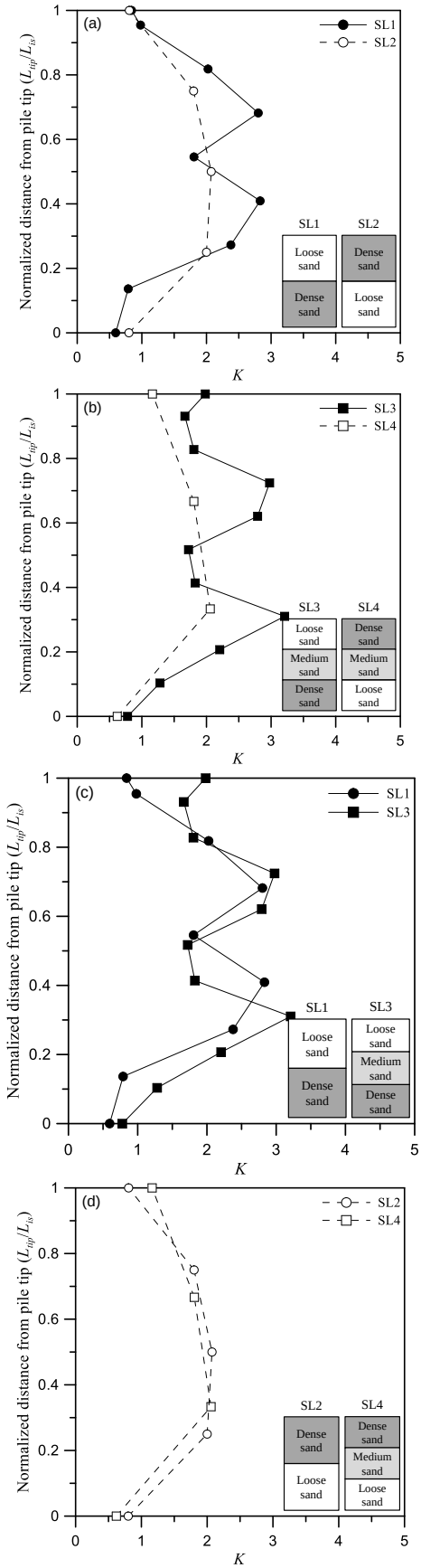

Fig. 12 Variations of K for different layering conditions versus normalized distance from pile tip L_{tip}/L_{is}: (a) SL1 & SL2, (b) SL3 & SL4, (c) SL1 & SL3, (d) SL2 & SL4 and (e) SL5 & SL6

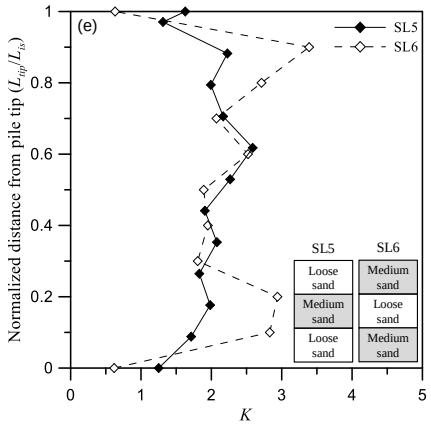

Fig. 12 Continued

As mentioned earlier, soil plugging of an open-ended pipe pile is influenced by pile diameter, soil conditions, and installation method. This study has focused only on the role of soil conditions and presents significant efforts to quantify the effect of soil conditions on the degree of soil plugging in terms of coefficient of lateral earth pressure inside the pile. The results from the numerical simulations performed in this study provide invaluable insights and may serve as numerical solutions to develop advanced theory for analysis and design of open-ended pipe piles, especially for estimation of inner shaft resistance after pile driving.

6. Conclusions

Large-deformation, 3D finite-element analyses were performed to investigate the effect of soil conditions on plugging of open-ended piles using the CEL technique. Results from the numerical model were compared against those from high-quality field load tests and showed very good agreement in terms of *PLR* and *SPI*. A parametric study was then performed on an open-ended steel pipe pile with an outer diameter of 0.5 m and a wall thickness of 10 mm, driven to a depth of 15 m for various soil conditions using the CEL model. Particular emphases were placed on investigating the variations of coefficient of lateral earth pressure in the soil plug after pile driving for various soil conditions. The following conclusions were drawn from the parametric study:

• Lengths of the soil plug L_s at the end of pile driving process obtained from the CEL analysis were 6.75, 9.75, and 10.95 m for loose, medium dense, and dense sands, respectively, corresponding to *PLR* values of 0.45, 0.65, and 0.73, respectively. The trend of increasing *PLR* with increasing density of soil was in good agreement with the previous experimental studies.

• Analysis results showed that K values were close to initial value (K_0 = 0.4) or slightly larger than the initial value but still smaller than 1 for upper portion of the soil plug. Then, the K values started to increase and reached maximum values that are greater than 1 near the pile base and decreased toward the pile base. The maximum K values

observed within the soil plug for loose, medium dense, and dense sands were 1.6, 2.5, and 3.2 showing increasing trend with increasing density. The maximum K values for each soil density corresponded to about 63%, 70%, and 71% of the coefficient K_p of passive earth pressure, respectively.

• The end-bearing conditions showed very little difference in K values for the bottom one third of the mobilized soil plug ($0 < L_{tip}/L_{is} < 0.3$) and top one third ($0.7 < L_{tip}/L_{is} < 1.0$). However, for the middle portion of the mobilized soil plug ($0.3 < L_{tip}/L_{is} < 0.7$), the K values generally increased with the increasing embedment length in the bearing layer, indicating that the end-bearing piles have more influence on the degree of soil plugging than the floating piles.

• For layered soil profiles, regardless of number of soil layers, the greater K values were obtained when the denser soil was located near the pile base. Furthermore, the K values for the soil conditions where the density increases with increasing depth showed two local maximum values at about L_{tip}/L_{is} of 0.35 and 0.7. On the other hand, the soil conditions where the density decreases with increasing depth did not show this behavior, having only one local maximum at the location near the bottom portion of the mobilized soil plug.

Acknowledgments

This work was supported by the National Research Foundation of Korea (NRF) grant funded by the Korea government (MSIT) (No. 2020R1F1A1076193 and 2022R1C1C1011477).

References

American Petroleum Institute (2011), *Geotechnical and Foundation Design Considerations: ANSI/API Recommended Practice 2GEO/ISO 19901-4. 1st Ed.*, American Petroleum Institute, Washington, DC, USA.

Bienen, B., Qiu, G. and Pucker, T. (2015), "CPT correlation developed from numerical analysis to predict jack-up foundation penetration into sand overlying clay", *Ocean. Eng.*, **108**, 216-226. https://doi.org/10.1016/j.oceaneng.2015.08.009.

Brown, D.A. and Thompson, W.R. (2015), *NCHRP Synthesis 478, Design and Load Testing of Large Diameter Open-Ended Driven Piles*. Transportation Research Board, National Academies, Washington, DC, USA.

Brucy, F., Meunier, J. and Nauroy, J.F. (1991), "Behavior of pile plug in sandy soil during and after driving", *Proceedings of the 23rd Annual Offshore Technology Conference*, Houston, TX, USA, May.

Caltrans (2015), *Technical Guidance for Assessment and Mitigation of the Hydroacoustic Effects of Pile Driving on Fish*, California Department of Transportation, Sacramento, USA.

Chen, F., Lin, Y., Dong, Y. and Li, D. (2020), "Numerical investigations of soil plugging effect inside large-diameter, open-ended wind turbine monopiles driven by vibratory hammers", *Mar. Georesour. Geotech.*, **38**, 83-96. https://doi.org/10.1080/1064119X.2018.1553081.

Dassault Systemes (2018), *Abaqus 2018 Online Documentation*, Simulia Corp., Providence, USA.

De Nicola, A. and Randolph, M.F. (1997), "The plugging behaviour of driven and jacked piles in sand", *Geotechnique*, **47**(4), 841-856. https://doi.org/10.1680/geot.1997.47.4.841.

Fattah, M.Y. and Al-Soudani, W.H.S. (2016), "Bearing capacity of open-ended pipe piles with restricted soil plug", *Ships Offshore Struct.*, **11**(5), 501-516. https://doi.org/10.1080/17445302.2015.1030247.

Goble, G.G., Raushe, F.R. and Likins, G.E. (1980), "The analysis of pile driving-a state-of-the-art", *Proceedings of International Seminar on the Application of Stress-Wave Theory on Piles*, Stockholm, Sweden, June.

Gudavalli, S.R., Safaqah, O. and Seo, H. (2013), "Effect of Soil Plugging on Axial Capacity of Open-Ended Pipe Piles in Sands", *Proceedings of the 18th International Conference on Soil Mechanics and Geotechnical Engineering*, Paris, France, September.

Gupta, T., Chakraborty, T., Abdel-Rahman, K. and Achmus, M. (2016), "Large Deformation Finite Element Analysis of Static Cone Penetration Test", *Indian Geotech. J.*, **46**(2), 115-123. https://doi.org/10.1007/s40098-015-0157-3.

Hsu, C.Y., Liang, C.C., Teng, T.L. and Nguyen, A.T. (2013), "A numerical study on high-speed water jet impact", *Ocean Eng.*, **72**, 98-106. https://doi.org/10.1016/j.oceaneng.2013.06.012.

Igoe, D.J.P., Gavin, K.G. and O'Kelly, B.C. (2008), "Field measurements of the base resistance of pipe piles in medium dense sand", *Proceedings of the Second BGA International Conference on Foundations (ICOF 2008)*, Dundee, Scotland, June.

Igoe, D., Doherty, P. and Gavin, K. (2010), "The Development and Testing of an Instrumented Open-Ended Model Pile", *Geotech. Test J.*, **33**(1), 72-82. https://doi.org/10.1520/GTJ102708.

Jeong, S., Ko, J., Won, J. and Lee, K. (2015), "Bearing capacity analysis of open-ended piles considering the degree of soil plugging", *Soil Found.*, **55**(5), 1001-1014. https://doi.org/10.1016/j.sandf.2015.06.007.

Kikuchi, Y., Mizutani, T., Morikawa, Y. and Sato, T. (2009), "Plugging Mechanism of open-ended piles", *Proceedings of the 17th International Conference on Soil Mechanics and Geotechnical Engineering,* Alexandria, Egypt, October.

Kim, D. and Jeong, S. (2021), "Estimation of the excavation damage zone in TBM tunnel using large deformation FE analysis", *Geomech. Eng.*, **24**(4), 323-335. https://doi.org/10.12989/gae.2021.24.4.323.

Kim, Y.H., Hossain, M.S. and Wang, D. (2015a), "Effect of strain rate and strain softening on embedment depth of a torpedo anchor in clay", *Ocean Eng.*, **108**, 704-715. https://doi.org/10.1016/j.oceaneng.2015.07.067.

Kim, Y.H., Hossain, M.S., Wang, D. and Randolph, M.F. (2015b), "Numerical investigation of dynamic installation of torpedo anchors", *Ocean Eng.*, **108**, 820-832. https://doi.org/10.1016/j.oceaneng.2015.08.033.

Kishida, H. and Isemoto, N. (1977), "Behavior of sand plugs in open ended steel pipe piles", *Proceedings of the 9th International Conference on Soil Mechanics and Foundation Engineering*, Tokyo, Japan, July.

Klos, J. and Tejchman, A. (1981), "Bearing capacity calculation for pipe piles", *Proceedings of the 10th International Conference on Soil Mechanics and Foundation Engineering*, Stockholm, Sweden, June.

Ko, J. and Jeong, S. (2015), "Plugging effect of open-ended piles in sandy soil", *Can. Geotech. J.*, **52**(5), 535-547. https://doi.org/10.1139/cgj-2014-0041.

Ko, J., Jeong, S. and Lee, J.K. (2016), "Large deformation FE analysis of driven steel pipe piles with soil plugging", *Comput. Geotech.,* **71**, 82-97. https://doi.org/10.1016/j.compgeo.2015.08.005.

Kodsy, A. and Iskander, M. (2022), "Insight into plugging of pipe piles based on pile dimensions", Appl. Sci., **12**, 2711.

https://doi.org/10.3390/app12052711.

Kraft, L.M. (1991), "Performance of axially loaded pipe piles in sand", *J. Geotech. Eng.*, **117**(2), 272-296. https://doi.org/10.1061/(ASCE)0733-9410(1991)117:2(272).

Lai, F., Liu, S., Deng, Y., Sun, Y., Wu, K. and Liu, H. (2020), "Numerical investigations of the installation process of giant deep-buried circular open caissons in undrained clay", *Comput. Geotech.*, **118**, 103322. https://doi.org/10.1016/j.compgeo.2019.103322.

Lee, K. and Jeong, S. (2018), "Large deformation FE analysis of a debris flow with entrainment of the soil layer", *Comput. Geotech.*, **96**, 258-268. https://doi.org/10.1016/j.compgeo.2017.11.008.

Lee, K., Kim, Y., Ko, J. and Jeong, S. (2019), "A study on the debris flow-induced impact force on check dam with- and without-entrainment", *Comput. Geotech.*, **113**, 103104. https://doi.org/10.1016/j.compgeo.2019.103104.

Lehane, B.M., Schneider, J.A. and Xu, X. (2005), "The UWA-05 method for prediction of axial capacity of driven piles in sand", *Proceedings of the International Symposium on Frontiers in Offshore Geotechnics (IS-FOG 2005)*, Perth, Australia, September.

Mabsout, M.E., Reese, L.C. and Tassoulas, J.L. (1995), "Study of pile driving by finite-element method", *J. Geotech. Eng.*, **121**(7), 535-543. https://doi.org/10.1061/(ASCE)0733-9410(1995)121:7(535).

Mabsout, M.E., Sadek, S.M. and Smayra, T.E. (1999), "Pile driving by numerical cavity expansion", *Int. J. Numer. Anal. Meth. Geomech.*, **23**(11), 1121-1140. https://doi.org/10.1002/(SICI)1096-9853(199909)23:11<1121::AID-NAG28>3.0.CO;2-Y.

Malhotra, S. (2002), "Axial load capacity of pipe piles in sand: revisited", *Proceedings of International Deep Foundations Congress 2002*, Orlando, FL, USA, February.

Paik, K.H. and Lee, S.R. (1993), "Behavior of soil plugs in open-ended model piles driven into sands", *Mar. Georesour. Geotech.,* **11**, 353-373. https://doi.org/10.1080/10641199309379929.

Paik, K. and Salgado, R. (2003), "Determination of bearing capacity of open-ended piles in sand", *J. Geotech. Geoenv. Eng.*, **129**(1), 46-57. https://doi.org/10.1061/(ASCE)1090-0241(2003)129:1(46).

Paik, K. and Salgado, R. (2004), "Effect of Pile Installation Method on Pipe Pile Behavior in Sands", *Geotech. Test. J.*, **27**(1), 1-11. https://doi.org/10.1520/GTJ11268J

Paikowsky, S.G. (1989), "A static evaluation of soil plug behaviour with application to the pile plugging problem", ScD. Dissertation, Massachusetts Institute of Technology, Cambridge, USA.

Paikowsky, S.G. (1990), "The mechanism of pile plugging in sand", *Proceedings of the 22nd Offshore Technology Conference*, Houston, TX, USA, May.

Pucker, T. and Grabe, J. (2012), "Numerical simulation of the installation process of full displacement piles", *Comput. Geotech.*, **45**, 93-106. https://doi.org/10.1016/j.compgeo.2012.05.006.

Qiu, G., Henke, S. and Grabe, J. (2011), "Application of a Coupled Eulerian-Lagrangian approach on geomechanical problems involving large deformations", *Comput. Geotech.*, **38**, 30-39. https://doi.org/10.1016/j.compgeo.2010.09.002.

Randolph, M.F., Leong, E.C. and Houlsby, G.T. (1991), "One-dimensional analysis of soil plugs in pipe piles", *Geotechnique*, **41**(4), 587-598. https://doi.org/10.1680/geot.1991.41.4.587.

Randolph, M.F., May, M., Leong, E.C., Hyden, A.M. and Murff, J.D. (1992), "Soil plug response in open ended pipe piles", *J. Geotech. Eng.*, **118**(5), 743-759. https://doi.org/10.1061/(ASCE)0733-9410(1992)118:5(743).

Randolph, M.F. and Wroth, C.P. (1981), "Application of the failure state in undrained simple shear to the shaft capacity of driven piles", *Geotechnique*, **31**(1), 143-157. https://doi.org/10.1680/geot.1981.31.1.143.

Rauche, F. (2000), "Keynote lecture: Pile driving equipment: Capabilities and properties", *Proceedings of the 6th International Conference on the Application of Stress-Wave Theory to Piles*, Sao Paulo, Brazil, September.

Seo, H. and Kim, M. (2017), "Soil plug behavior of open-ended pipe piles during installation", *DFI Journal - The Journal of the Deep Foundations Institute*, **11**(2-3), 128-136. https://doi.org/10.1080/19375247.2018.1448552.

Szechy, C.H. (1959), "Tests with tubular piles", Acta Technica. 24, 181-219.

Tho, K.K., Leung, C.F., Chow, Y.K. and Swaddiwudhipong, S. (2012), "Eulerian finite-element technique for analysis of jack-up spudcan penetration", *J. Geotech. Geoenv. Eng.*, **12**(1), 64-73. https://doi.org/10.1061/(ASCE)GM.1943-5622.0000111.

Tho, K.K., Chen, Z., Leung, C.F. and Chow, Y.K. (2014), "Enhanced analysis of pile flexural behaviour due to installation of adjacent pile", *Can. Geotech. J.*, **51**(6), 705-711. https://doi.org/10.1139/cgj-2013-0215.

Tolooiyan, A. and Gavin, K. (2011), "Modelling the cone penetration test in sand using cavity expansion and arbitrary Lagrangian Eulerian finite element methods", *Comput. Geotech.*, **38**, 482–490. https://doi.org/10.1016/j.compgeo.2011.02.012.

White, D.J., Schneider, J.A. and Lehane, B.M. (2005), "The influence of effective area ratio on shaft friction of displacement piles in sand", *Proceedings of the International Symposium on Frontiers in Offshore Geotechnics (IS-FOG 2005)*, Perth, Australia, September.

Yamahara, H. (1964), "Plugging effects and bearing mechanism of steel pipe piles", *Transportation of the Architectural Institute of Japan*, **96**, 28-35.

Yi, J.T., Lee, F.H., Goh, S.H., Zhang, X.Y. and Wu, J.F. (2012), "Eulerian finite element analysis of excess pore pressure generated by spudcan installation into soft clay", *Comput. Geotech.*, **42**, 157-170. https://doi.org/10.1016/j.compgeo.2012.01.006.

Yu, F. and Yang, M. (2012), "Base Capacity of Open-Ended Steel Pipe Piles in Sand", *J. Geotech. Geoenv. Eng.*, **138**(9), 1116 – 1128. https://doi.org/10.1061/(ASCE)GT.1943-5606.0000667.

Zhao, Y. and Liu, H. (2015), "The drag effects on the penetration behavior of drag anchors during installation", *Ocean Eng.,* **109**, 169-180. https://doi.org/10.1016/j.oceaneng.2015.09.011.

IC

Notation

The following symbols are used in this paper:

$A_{b,ann}$	annular area of pile base
$A_{b,plug}$	cross-sectional area of soil plug
$A_{s,in}$	inner surface area of pile-soil interface (= $\pi B_i L_{is}$)
$A_{s,out}$	outer surface area of pile-soil interface (= $\pi B_o L_p$)
B_i	pile inner diameter
B_o	pile outer diameter
C_c	coefficient of curvature
C_u	coefficient of uniformity
c	cohesion
E	elastic modulus
E_E	elastic modulus of end bearing layer
G_s	specific gravity
IFR	incremental filling ratio
K	coefficient of lateral earth pressure (where $K = \sigma'_h / \sigma'_v$)
K_0	coefficient of lateral earth pressure at rest (K_0 = 1-sinϕ)
K_p	coefficient of passive earth pressure ($K_p = (1+\sin\phi)/(1-\sin\phi)$)
L	pile length
L_{is}	length of the soil plug along which inner shaft resistance is mobilized
L_p	pile penetration depth
L_s	soil plug length
L_{tip}	distance from the pile tip
N	standard penetration number
N_q	end bearing factor
PLR	plug length ratio
Q_{ann}	annulus resistance
Q_{base}	end bearing resistance
Q_{in}	inner shaft resistance
Q_{out}	outer shaft resistance
Q_{plug}	soil pug resistance
Q_{ult}	ultimate capacity
q_b	unit end bearing resistance
q_s	unit shaft resistance
$q_{s,in}$	unit inner shaft resistance
$q_{s,out}$	unit outer shaft resistance
R	pile radius
SPI	soil plugging index
t	pile thickness
$z_{bearing}$	depth to the top of the bearing layer below ground surface
β	shaft friction factor
ΔL_p	increment of pile penetration depth
ΔL_s	increment of soil plug length
δ	soil-pile interface friction angle
δ_r	relative displacement of radial soil flow
γ_t	Total unit weight
μ	friction coefficient
v	Poisson's ratio
σ'_h	horizontal effective stress
σ'_v	vertical effective stress
σ'_{vb}	vertical effective stress at the pile base
σ_1	major principal stress
σ_3	minor principal stress
ϕ	peak friction angle
ϕ_E	peak friction angle of end bearing layer